Agricultural and Forest Meteorology 287 (2020) 107930

Contents lists available at ScienceDirect

Agricultural and Forest Meteorology

journal homepage: www.elsevier.com/locate/agrformet

Research paper

Redefining droughts for the U.S. Corn Belt: The dominant role of atmospheric vapor pressure deficit over soil moisture in regulating stomatal behavior of Maize and Soybean

Hyungsuk Kimm[a,*], Kaiyu Guan[a,b,*], Pierre Gentine[c], Jin Wu[d,e], Carl J. Bernacchi[f,g], Benjamin N. Sulman[h,i], Timothy J. Griffis[j], Changjie Lin[k]

[a] College of Agricultural, Consumer and Environmental Sciences, University of Illinois at Urbana-Champaign, Urbana, IL, United States
[b] National Center for Supercomputing Applications, University of Illinois at Urbana-Champaign, Urbana, Illinois, United States
[c] Department of Earth and Environmental Engineering, Columbia University, New York, New York, United States
[d] Brookhaven National Laboratory, Environmental & Climate Sciences Department, New York, New York, United States
[e] School of Biological Sciences, University of Hong Kong, Pokfulam, Hong Kong
[f] USDA-ARS Global Change and Photosynthesis Research Unit, Urbana, IL, United States
[g] Department of Plant Biology, the University of Illinois at Urbana-Champaign, Urbana, Illinois, United States
[h] Department of Geosciences, Princeton University, Princeton, NJ, United States
[i] School of Natural Sciences, University of California, Merced, United States
[j] Department of Soil, Water, and Climate, University of Minnesota, Saint Paul, Minnesota, United States
[k] State Key Laboratory of Hydroscience and Engineering, Department of Hydraulic Engineering, Tsinghua University, Beijing, China

ARTICLE INFO

Keywords:
Agroecosystem
Agricultural drought
Ecosystem stomatal conductance
Vapor pressure deficit
Soil water content

ABSTRACT

The U.S. Corn Belt, the world's biggest production region for corn and soybean combined, is prone to droughts. Currently 92% of the U.S. Corn Belt croplands are rainfed, and thus are sensitive to interannual climate variability and future climate change. Most prior studies identify the lack of soil moisture as the primary cause of agricultural drought impacts, although water-related stresses are also induced by high atmospheric water demands (i.e., vapor pressure deficit, VPD). Here we empirically attributed the variability of canopy-level stomatal conductance (Gs) and gross primary productivity (GPP) to VPD and soil water supply (i.e. volumetric soil water content, SWC), using eddy-covariance data from seven AmeriFlux eddy covariance sites in maize and soybean fields across the U.S. Corn Belt, which are well represented for the current rainfed part of the Corn Belt croplands. We used three independent approaches, including two statistical models (i.e. a multiple-linear regression model and a semi-empirical, non-linear model) and information theory, to quantify the relationship of Gs (or GPP) with VPD and SWC. The attribution result from the two models shows that VPD explains most of Gs variability (91% and 89%, respectively), and mutual information also attributed 91% of GPP variability to VPD. This finding was robust over the gradients of rainfall and temperature, crop types (maize vs. soybean), and management practices (whether irrigated or not). We reconciled our finding with the previously emphasized importance of precipitation and SWC, by conducting a path analysis, which revealed the causal relationships between precipitation, air temperature (Ta), relative humidity (RH), VPD, SWC, and Gs. We find that precipitation impacts on Gs through reduced RH and Ta to VPD (rather than directly through SWC). With increased VPD robustly projected under climate change, we expect increased crop water stress in the future for the U.S. Corn Belt.

1. Introduction

Agricultural drought has been defined mostly by precipitation shortage (Mishra et al., 2010; Palmer, 1965; Panu and Sharma, 2002), or soil moisture deficiency (Mishra and Singh, 2010), while a greater number of studies rely on precipitation rather than on soil moisture (SM) because precipitation is a good proxy of soil water supply variations, and a continuous record of SM is often scarce, especially from the root zone (Heim, 2002; Palmer, 1965). However, plant hydraulic status is also largely affected by increase of atmospheric water demand

* Corresponding authors.
E-mail addresses: hk8@illinois.edu (H. Kimm), kaiyug@illinois.edu (K. Guan).

https://doi.org/10.1016/j.agrformet.2020.107930
Received 8 August 2019; Received in revised form 13 December 2019; Accepted 2 February 2020

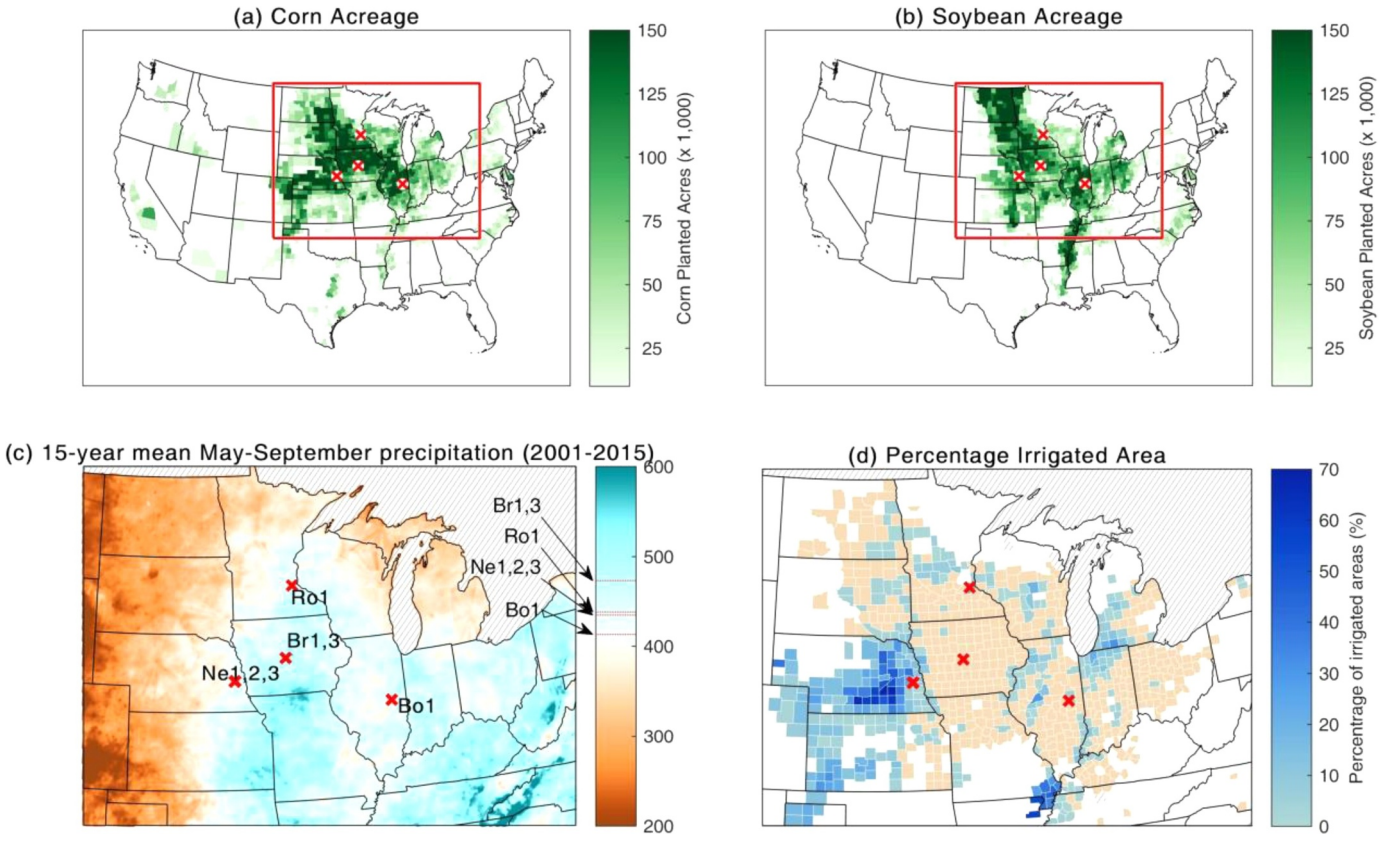

Fig. 1. (a) A County level map of corn-planted acreage (corn for all purposes) and (b) soybean-planted acreage in 2017 based on the Crop Acreage Data from USDA. A red-colored box indicates the majority of the U.S. Corn Belt area, which is used to generate the panels (c) and (d). The bottom panels show (c) the spatial pattern of 15 years mean May-to-September precipitation and (d) irrigated and rainfed areas in 2012 where brown areas are rain-fed (< 1% irrigated area) and colors indicates the percentage of irrigated areas. Precipitation data are from PRISM climate data (http://www.prism.oregonstate.edu/), and the irrigated area data are from MODIS-based Irrigated Agriculture Dataset (https://earlywarning.usgs.gov/USirrigation). Cross marks are indicating locations of the flux tower sites of the study. Site names are marked in panel (c) at the corresponding locations and color codes. Outside the U.S. and lakes are patterned with stripes. .

(Anderson et al., 2010; Lobell et al., 2014; Wilhite and Glantz, 1985). The key behind these impacts from different factors is plant stomatal behavior (Chaves et al., 2003). Stomata control gas exchanges (i.e., CO_2 uptake and water vapor loss) at leaf surface, and stomatal regulations can be primarily attributed to two factors, increased atmospheric water demand and decreased soil water supply (Katul et al., 2012; Oren et al., 1999). Atmospheric water demand, which is practically characterized by the atmospheric vapor pressure deficit (VPD) is a major driving force of transpiration; and under high VPD conditions, plants tend to close their stomata which restricts photosynthetic activities (Monteith, 1995). Regarding SM deficiency, plant xylems or plants' roots sense low water supply which induces stomatal closure and reduces photosynthesis and water loss (Huang et al., 2016; Martínez-Vilalta et al., 2014; Sadras and Milroy, 1996; Taiz et al., 2014).

The aforementioned two major pathways of stomatal regulation, dry air and dry soils, are often tightly coupled. For example, the lack of precipitation does not only lead to SM deficit, but also increases VPD through land-atmosphere interactions which increase temperature and decrease specific humidity (Gentine et al., 2016; Green et al., 2017). Strong tendency of co-occurrence of droughts and heat waves in the U.S. also supports the strong coupling between precipitation, soil moisture and VPD (Chang and Wallace, 1987; Peterson et al., 2013; Trenberth et al., 1988). Therefore, it is important to disentangle the relative importance of VPD and SM in controlling stomatal behavior during drought conditions. Recent studies have explored to what extent VPD and SM control stomatal behavior and metabolic processes in natural ecosystems, by employing parsimonious approaches to isolate and quantify the relative impacts of VPD and SWC on plants using the Ameriflux eddy-covariance flux tower network. Novick et al. (2016) evaluated the impact of VPD and SWC on canopy-level stomatal conductance (Gs) and evapotranspiration (ET) and suggested an increasing impact of VPD on ET with temperature increase under climate change scenarios. Sulman et al. (2016) analyzed a 13-year record of flux tower data and evaluated inter-annual variability of influences of VPD and SWC on gross primary productivity (GPP) and ET, and suggested that VPD was the primary contributor though SWC contributed as much as VPD in a severe drought year. Lin et al. (2018) analyzed a suite of available FLUXNET data across various biomes and found that VPD dominates Gs at sub-daily timescales with limited soil moisture impacts at least in non-extreme drought conditions. However, less work has been done specifically on agroecosystems where understanding of drought is important, not only due to the vast area of agroecosystems but also to food production and security. A better understanding of agricultural drought would be broadly applicable, and helpful to understand sensitivity of yield to environmental factors in the current and future climate.

There exist advanced approaches beyond regression modeling that can quantify causal relationships. The notable approaches include wavelet analysis and information theory, or a combination of the two (Sturtevant et al., 2016). Wavelet analysis has been extensively used in bio-signal interpretation such as electrocardiogram to separate a time-series signal into multiple frequencies of information. Several studies of biophysics and Earth sciences have adopted this to address timescale-dependent issues (Dietze et al., 2011; Guan et al., 2011; Stoy et al., 2005). Further, information theory, which utilizes Shannon entropy (Shannon, 1948), has emerged as an alternative analysis accounting for

the non-linear characteristics of data. Information theory quantifies "information" contained in a random variable and is often used to address relationships between the amount of information and spatial resolution (Brunsell and Anderson, 2011; Stoy et al., 2009). Furthermore, some of the information theory methods such as mutual information and transfer entropy apply to quantification of causal relationships between biophysical and meteorological variables (Kumar and Ruddell, 2010; Sturtevant et al., 2016), yet such application is relatively new and rare in this research domain.

This study specifically focuses on the U.S. Corn Belt, which produces ~40% and ~30% of global production of maize and soybean, respectively (FAO, 2013), and thus plays a critical role in the regional economy and global food security (Guan et al., 2016; Lobell et al., 2014). In this study, we examine the relative contributions of VPD and SWC to variations in Gs for the U.S. Corn Belt agroecosystem using seven eddy-covariance flux towers spanning the four major Corn Belt states, including Nebraska, Minnesota, Iowa, and Illinois (Fig. 1). Lobell et al. (2014) showed an increasing pattern of yield variability in the U.S. Corn Belt, and VPD was a major contributor to such variability. Additionally, we show that the large variability in County level crop yield data is up to 25% compared to 30-year mean crop yield, and this implies the importance of understanding crop physiological mechanism of crop water stress in the region (Figure S1). We used eddy-covariance data covering varying periods from 1997 to 2012 to fit models of Gs as a function of VPD and SWC. Specifically, we address the following three science questions: (1) How well can empirical models using VPD and SWC explain the variability of Gs in croplands? (2) What are the relative contributions of VPD and SWC to plant water stress in croplands? (3) What are the implications of our findings in defining and characterizing the agricultural drought effects for the US Corn Belt?

2. Materials and methods

2.1. Data

This study includes all available Ameriflux sites (seven sites) within the U.S. Corn Belt where soil moisture data (SWC from 10–25 cm depth) are available for more than 4 years. Sites are from the four major U.S. Corn Belt states, i.e. Illinois, Iowa, Nebraska, and Minnesota. Based on the National Agricultural Statistics Service's statistics from the U.S. Department of Agriculture, these four states (Illinois, Iowa, Nebraska, and Minnesota) produced 16%, 16%, 12% and 10% of the U.S. Corn and 15%, 16%, 7%, and 9% of the U.S. soybean production, respectively, during the period of 1996–2012. Two sites in Nebraska are irrigated, and the rest of the sites are rain-fed. The study sites span a rainfall gradient from 283 mm to 623 mm per growing season (May-Sep), but with a relatively small temperature gradient (18.89 °C – 21.22 °C of mean air temperature during the growing season). The rainfall gradient across the sites allows us to compare the results with respect to the dry-wet condition. The sites also enable us to compare two different crops (maize vs. soybean) as well as water management practices (rain-fed vs. irrigated). At most sites, maize and soybean are rotationally planted, and considering the significant difference in plant physiology between maize and soybean, we separated the dataset into maize years and soybean years (Table 1). Including this crop separation, we have 11 cases in total. In Table 1, we provided aridity index next to site names as a proxy of dryness, which is calculated as the ratio of annual mean precipitation divided by annual mean potential evaporation (Allen et al., 1998)

2.2. Overview of the methodology

To address the questions raised above, we used three different and independent approaches, including a multiple linear regression model, a non-linear model, and mutual information combined with wavelet analysis. With regards to the first two approaches, we first derived Gs using multiple eddy-covariance flux tower data by inverting the Penman-Monteith equation. Second, relationships among VPD, SWC, and Gs were evaluated at hourly, daily and weekly timescales to decide an appropriate timescale for the analyses. Third, we developed two different empirical models of Gs using VPD and SWC as the explanatory variables. The two models are a multiple linear regression and a non-linear model, with further details introduced in *Section 2.4*. Variation in Gs was attributed to VPD and SWC by using an analysis of variance (ANOVA) for the linear model and numerically calculated partial derivatives for the non-linear model. Regarding the third approach, we first use the wavelet analysis to decompose the gap-filled time-series of VPD, SWC, and GPP (See *approach 3* in the Materials and Methods, for further description about why we use GPP here instead of Gs) into multiple frequencies of information, and reconstructed at three timescales, hourly, diel, and multiday scales. Second, based on the reconstructed time-series data, we quantified mutual information, i.e., the amount of shared information between the variables on a basis of Shannon's entropy, and regarded it as the contributions of VPD and SWC to GPP. Finally, to reconcile results from these analyses with pre-existing knowledge about the impact of environmental factors on agricultural drought impacts, we used a path analysis that quantifies the causation between multiple variables of interests, with prior knowledge-based path structure (Li, 1975; Wu et al., 2016).

2.3. Approaches 1 & 2: deriving canopy-level stomatal conductance from flux tower-measured Et

Following the approach of Novick et al. (2016), we used the Penman-Monteith equation to derive canopy-level stomatal conductance from flux tower data (Monteith, 1965). To avoid inconsistent patterns (lower stomatal conductance with higher soil moisture; Figure S2), and to account for occurrence probability of a specific environmental condition, we used the data without stratification. Since the flux tower-measured ET combines transpiration and evaporation, to minimize the soil evaporation effects, we only used the data from July and August, which belong to the peak growing season for the US Corn Belt and enable us to assume that maize and soybean canopies are closed. To minimize the effects of evaporation from canopy interception, we excluded data within two days following every precipitation and irrigation event. Furthermore, we excluded periods of low incoming shortwave radiation (SR_{in}) conditions (<500 Wm^{-2}) to avoid including morning dew formation and evaporation on the plant surface, and to restrict the analysis to light saturated conditions. After we applied the data filters, stomatal conductance was derived by inverting the Penman-Monteith equation (Eq. (1)) as shown in Eq. (2:)

$$\lambda E = \frac{\Delta(R_n - G) + \rho C_p g_a (e_s(T_a) - e_a)}{\Delta + \gamma(1 + g_a/Gs)} \quad (1)$$

$$Gs = g_a \gamma / \left\{ \frac{\Delta(R_n - G) + \rho C_p g_a (e_s(T_a) - e_a)}{\lambda E} - (\Delta + \gamma) \right\} \quad (2)$$

where Gs and g_a are canopy stomatal conductance and aerodynamic conductance, γ is the psychometric constant, Δ is the slope of the water vapor deficit, R_n and G are net radiation and soil heat flux, ρ is air density, C_p is specific heat capacity of dry air, e_s and e_a are saturated and actual vapor pressure, T_a is air temperature, and λE is evapotranspiration.

2.4. Approaches 1 & 2: attributing the controls of VPD and SWC on stomatal conductance: two approaches

Before we developed models to attribute the VPD and SWC impacts on Gs, we first looked at the correlations between Gs, VPD and SWC at various timescales (from hourly, daily, weekly, to monthly), to identify the proper timescale for model fitting as well as attribution analysis.

Table 1
Site information.

Site (aridity index)	Crop	Years	MAP (May-Sep)	MAT (May-Sep)	Management	Reference
US-Bo1 (0.82)	Maize	Odd years during 1997–2007	363.22	21.03	Rainfed	(Meyers and Hollinger, 2004)
	Soybean	Even years during 1997–2007	285.76	20.91	Rainfed	
US-Br1 0.95)	Maize	2007, 2009, 2011	364.81	20.18	Rainfed	(Cammalleri et al., 2014)
	Soybean	2008, 2010	589.96	20.08	Rainfed	
US-Br3 (0.83)	Maize	2008, 2010	623.57	20.23	Rainfed	(Sakai et al., 2016)
	Soybean	2007, 2009, 2011	283.72	20.37	Rainfed	
US-Ne1 (0.73)	Maize	2001–2012	592.68	21.07	Irrigated	(Suyker et al., 2004)
US-Ne2(0.80)	Maize	Odd years during 2001–2009, and 2010–2012	572.22	21.05	Irrigated	(Suyker et al., 2004)
	Soybean	Even years during 2001–2008	607.16	20.70	Rainfed	
US-Ne3 (0.63)	Maize	Odd years during 2001–2012	369.09	21.22	Rainfed	(Suyker et al., 2004)
	Soybean	Even years during 2001–2012	469.78	21.02	Rainfed	
US-Ro1 (0.98)	Maize	Odd years during 2005–2011	482.64	18.89	Rainfed	(Fassbinder et al., 2012)

Then, we employed two empirical model approaches to model Gs, and to attribute the VPD and SWC impacts on Gs. Both models have been used in the previous literature for modeling Gs, or quantifying the effects of VPD and SWC on stomatal conductance.

The first model is a multiple linear regression used by Sulman et al. (2016) to quantify inter-annual trends in the attribution of GPP or ET variance to VPD and soil water potential (SWP) derived from an empirical relationship with SWC. Specifically, we fitted the following multiple linear regression with slight modification in the soil moisture and interaction terms:

$$Gs = c_1 \cdot \log(VPD) + c_2 \cdot SWC + c_3 \cdot \frac{SWC}{\log(VPD)} + c_4 \quad (3)$$

We used SWC instead of SWP, which was unavailable for our sites. However, a non-linear relationship between SWC and SWP was incorporated into our second model through a non-linear transformation of the SWC. While Sulman et al. (2016) used the multiplicative form of soil water potential (SWP) and log(VPD) as an interaction term we used the fractional form where both terms have positive impact on Gs because other forms of interaction term (*e.g.*, $\log(VPD) \cdot SWC$ or $\log(VDP)/SWC$) showed no significant contribution to explaining the variance of Gs. To attribute Gs variance to VPD and SWC using the above linear regression model, we conducted an analysis of variance (ANOVA). Contributions of VPD and SWC were defined as the ratios of each term's sum of squares (SS_{VPD} or SS_{SWC}) to the total (VPD and SWC) sum of square (SST). We forced contributions of VPD or SWC to be zero in cases for which they were insignificant ($P > 0.05$), or opposed to physiological understanding (e.g., increase of Gs under high VPD or low SWC).

The second approach is a non-linear and empirical relationship-based model which consists of two sub-functions, with one representing the non-linear relationships between Gs and VPD (i.e. the first term in the left-hand side of Eq. (4)), and the other representing the relationship between Gs and SWC (i.e. the second term in the right-hand side of Eq. (4)):

$$Gs = \left(\frac{a_1}{VPD - a_2} + a_3\right) \times \left(\frac{b_1}{1 + \exp(b_2(SWC - b_3))}\right) \quad (4)$$

where a_i ($i = 1, 2, 3$) and b_i ($i = 1, 2, 3$) are parameters to be fitted. The first component in Eq. (4) represents the relationship between VPD and Gs as an inverse proportional function, which has been widely confirmed in prior studies (Leuning, 1995; Lohammar et al., 1980). A recent study by Lin et al. (2018) found that the exponent of VPD can vary between 0.5 and 1 for different plant functional types, with a value close to 1 in croplands. The second component in Eq. (4) represents a logistic function between SWC and Gs, which has been proposed and validated by previous experimental studies (Davies and Zhang, 1991; Gollan et al., 1992). Once we fitted the second model, we numerically calculated normalized partial derivatives of the function with respect to VPD and SWC in order to attribute the variance of Gs to VPD and SWC. For a fair comparison between the effects of SWC and VPD, we first normalized VPD and SWC by calculating the standardized Z-score across a site-specific range of each variable. We calculated $\Delta Gs/\Delta VPD_{normalized}$ and $\Delta Gs/\Delta SWC_{normalized}$ over the actual ranges of VPD and SWC at an interval of one-eighth of a range. We set an arbitrary interval but the specific interval had no impact on the quantified partial derivatives as we normalized both VPD and SWC. Finally, we calculated total mean partial derivative values for both VPD and SWC.

The first model has a much simpler structure, and its linear nature makes it straightforward to calculate the statistical significance level for each variable of the regression model. However, since the sign of coefficients is not constrained in this simple statistical model, it can produce counter-intuitive responses, such as a positive relationship between Gs and VPD or a negative relationship between Gs and SWC, due to random variability in the data. This is thus the main drawback of the first approach.

The second approach is designed to incorporate the knowledge of plant physiology into the model and thus incorporates constraints for the relationship between VPD and Gs (only a negative relationship between VPD and Gs is allowed) and between SWC and Gs (a logistic-type of response is allowed, thus only a positive relationship between SWC and Gs is permitted). Furthermore, the second model reflects previously established non-linear relationships between the variables.

2.5. Approach 3: wavelet decomposition and quantification of mutual information

We adopted information theory combined with wavelet analysis following Sturtevant et al. (2016). Here, wavelet analysis requires gap-free data, but the derived Gs includes relatively large data gaps due to data filters and the number of variables involved in the Gs computation. Therefore, we chose GPP instead of Gs, as a dependent variable. GPP is determined both by Gs and by intercellular concentration of CO_2, which is a function of atmospheric CO_2 concentration and leaf photosynthetic and respiratory carbon metabolism. Therefore, the wavelet analysis on GPP does not directly translate to Gs. However, because the supply of CO_2, determined by Gs, is a critical component of GPP, and because wavelet analysis cannot be performed on Gs, we used GPP as a proxy for Gs. To further minimize the gaps and maximize the input data record, we used REddyProc R-package that fills gaps in VPD and Net ecosystem exchange (NEE), and partitions NEE into GPP and ecosystem respiration (Reco) (Reichstein et al., 2017; Wutzler et al., 2018). Regarding SWC, we used linear interpolation up to one week of gaps. Years with SWC gaps longer than one week within the peak growing season (July and August) were excluded from the analysis.

We then applied a wavelet analysis to decompose the gap-filled half-hourly time-series data into fourteen frequencies of information from 2^1 to 2^{14} scales (i.e., 1 h - 341 days) without data aggregation thus conserving the original number of data points. We used maximum overlap discrete wavelet transform (MODWT) rather than orthogonal discrete wavelet transform (DWT), as it produces more reliable and consistent results (D. P. Percival, 1995; Z. Zhang et al., 2016). Decomposed

wavelets were reconstructed from multi-frequency analysis (Mallat, 1989) at all levels, and then those were aggregated at three different timescales from hourly (2^1 to 2^2), diel (2^3 to 2^6), and multiday (2^7 to 2^{10}) scales. The entire wavelet analysis was conducted by using WMTSA Wavelet Toolkit of MATLAB that is based on Percival and Walden (2000).

Mutual Information (MI), based on the wavelets reconstructed at the three timescales, quantified the amount of shared information between the variables (i.e. VPD, SWC and GPP), at multiple frequencies (inverse of timescales) of information. The basis of MI is the Shannon entropy (H) that calculates the expected amount of unpredictability or information as a product of a probability of a certain event (p) and information conveyed by the event that equals -log (p) (Eq. (5); Shannon, 1948). A calculation of MI for two random variables, X and Y ($I_{X;Y}$), involves marginal entropies (Eq. (5)) and joint entropy (Eq. (6)) of two variables (Eq. (7)), i.e., "x = VPD, y = GPP" or "x = SWC and y = GPP". To quantify the contribution fractions of VPD and SWC, we calculated relative mutual information ($IR_{X;Y}$) by dividing $I_{X;Y}$ by a marginal entropy of the dependent variable (entropy of GPP = H_{GPP}; Eq. (8)).

$$Hx = -\sum_t p(x_t)\cdot\log(p(x_t)) \tag{5}$$

$$Hxy = -\sum_t (p(x_t, yt_t)\cdot\log(p(x_t, y_t))) \tag{6}$$

$$I_{X;Y} = Hx + Hy - Hxy \tag{7}$$

$$IR_{X;Y} = I_{X;Y}/Hy \tag{8}$$

Here, we only chose data from July and August to focus on peak growing season. We also utilized IR to quantify lag effects of VPD and SWC on GPP. IR value was computed at all specific lag intervals from 0 to 48 h at the diel timescale analysis, and from 0 to 10 days at the multiday timescale. When the highest IR achieved with a specific lag interval was found, we plotted the IR and the specific lag interval on top of IR with no lag effect (Fig. 8). All computations for IR were conducted by ProcessNetwork Software (version 1.5; Ruddell et al., 2008).

2.6. Path analysis

To characterize connections among environmental variables and Gs and determine sequential processes controlling Gs, we used a path analysis (Li, 1975). A path analysis uses a path structure that consists of variables of interest with potential connectivity among the variables where the connections are based on previously well-established knowledge (see Fig. 2). Based on the variables and the connections, a set of multiple linear regression models is constructed, and the partial regression coefficients are defined as path values (PV) that indicate the causative power of each connection. We prepared a path structure that includes variables such as precipitation (PPT), air temperature (Ta), VPD, SWC, and Gs. The connections in the structure include: (i) PPT (time since the latest precipitation) influences SWC, RH, and Ta, (ii) SWC affects Ta and RH, (iii) Ta and RH determine VPD, (iv) both VPD and SWC influence Gs, and (v) both Gs and VPD determine ET (Fig. 2). With Gs-related paths, we applied the same data filters used in the Gs derivation, and otherwise, only the growing season filter was applied. Regarding PPT, we used both precipitation amount and "time since the latest precipitation", but precipitation amount in all occasions was insignificant. To achieve a fair comparison among the path values of the connections, we standardized all variables prior to fitting the regression models. Then, we iteratively fitted regression models and eliminated insignificant factors ($P > 0.05$) in each trial. When there were only significant factors left, we obtained the partial regression coefficients as path values.

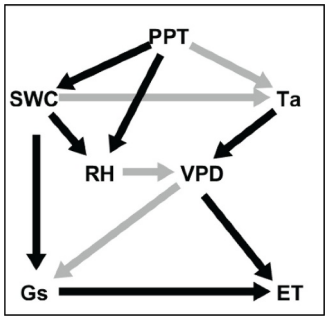

Fig. 2. Schematic diagram of a structure for the path analysis. Black lines indicate positive effects and gray lines indicate negative effects.

3. Results

3.1. Approaches 1 & 2: relationships among VPD, SWC, and GS across various timescales

Relationships among VPD, SWC, and Gs varied across different timescales. At a longer timescale, e.g., monthly scale, both VPD and SWC had a higher correlation with Gs, and VPD and SWC also had a higher correlation with each other (Fig. 3). Therefore, a shorter temporal resolution was necessary to disentangle effects of an individual factor on Gs. Further, both Gs and VPD have strong diurnal trends and thus their correlation at the hourly timescale is much higher than the correlation between Gs and SWC, as SWC is unlikely to have a diurnal trend. Diurnal variations in Gs are also strongly influenced by diurnal variations in SR_{in}. Therefore, we chose a daily scale that decouples VPD and SWC effects on Gs and removes the effect of the diurnal trends in VPD, Gs, and SR_{in} from the correlation between VPD and Gs.

3.2. Approaches 1 & 2: model fitting

We separately fitted the two empirical models (Eq. (3) and Eq. (4)) using the daily timescale data for maize years and soybean years at each site. Fitting performance varied across the 11 cases, as shown in Table 1, from $R^2 = 0.15$ to $R^2 = 0.67$ for the linear model fitting, and from 0.13 to 0.66 for the non-linear model fitting. Averaged model fitting performances across all the cases were $R^2 = 0.44$ and $R^2 = 0.42$ for the linear and non-linear models, respectively (Table. S1). Both models fit better with soybean than with maize (the linear model: $R^2 = 0.38$ for maize and $R^2 = 0.52$ for soybean; the non-linear model: $R^2 = 0.36$ for maize and $R^2 = 0.51$ for soybean). The four Br cases (Br1-maize, Br1-soybean, Br3-maize, and Br3-soybean) had the shortest data record (2–3 years; Table 1) and had the worst performance (R^2 ranged from 0.13 to 0.45). Without these Br cases, average performance increased to $R^2 = 0.55$ and $R^2 = 0.53$ respectively for the linear and non-linear models. Fig. 4 shows an example to illustrate the fitted response by the linear and non-linear models (see Figure S3 for all cases). The non-linear model generates a curved response surface of Gs relative to VPD and SWC, while the linear model generates a curved response to VPD and a linear response to SWC. Following a diagonal trajectory from low VPD, high SWC to high VPD, low SWC shows the effect of a strong coupling of VPD and SWC and their joint impacts on explaining the Gs variance. Statistically, such variance of Gs can be explained by either VPD or SWC, due to the strong coupling of these variables. The opposite diagonal trajectory of the surface, from low VPD, low SWC to high VPD, high SWC illustrates a situation in which VPD and SWC are decoupled. This enables us to differentiate the effects of VPD and SWC on Gs.

3.3. Approaches 1 & 2: attribution of GS variance to VPD and SWC

After we fitted the two empirical models using the daily timescale data, we used the ANOVA and partial derivative approaches to attribute the variance of Gs explained by VPD and SWC in the two models, respectively. Overall, the attribution analysis results consistently

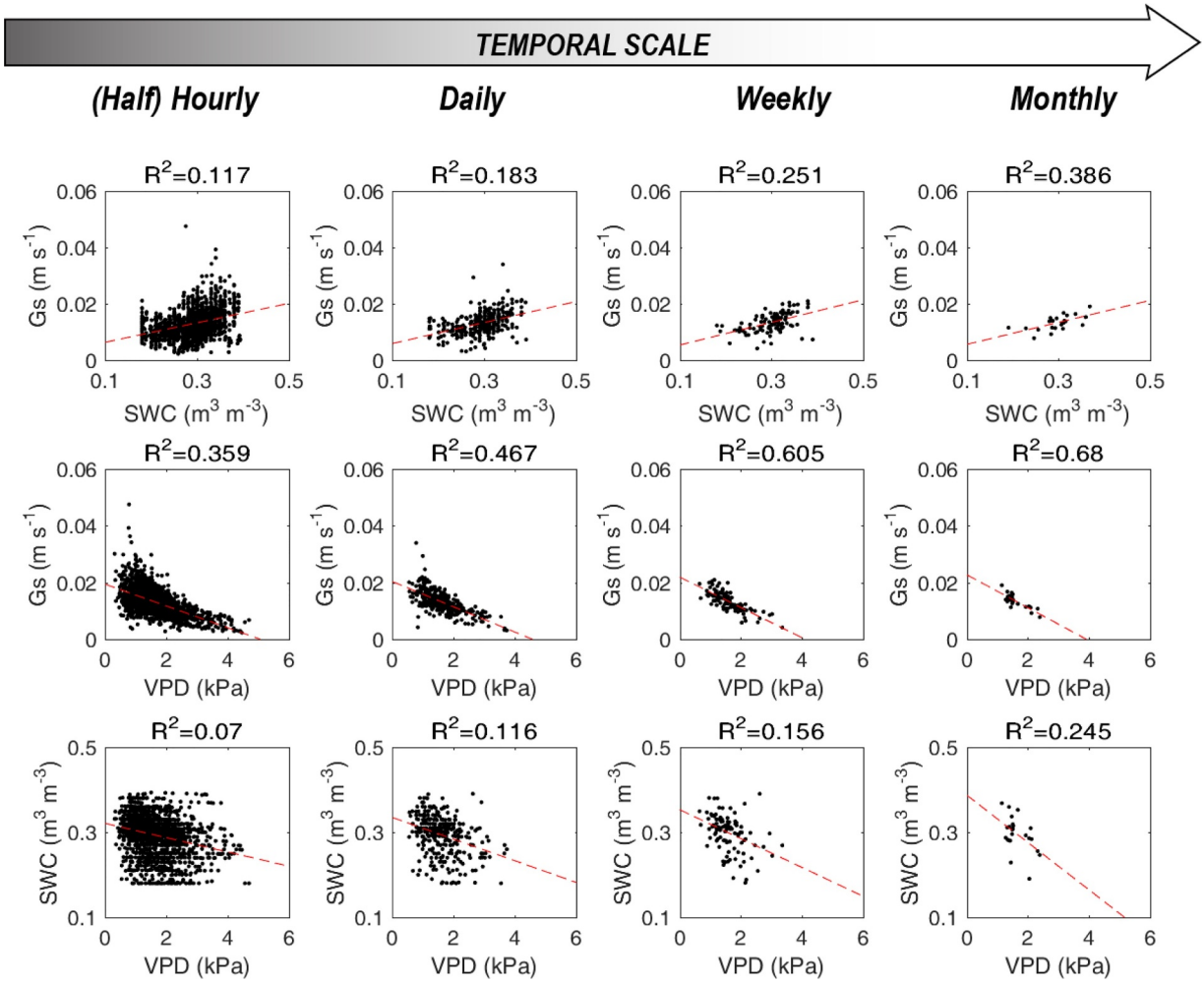

Fig. 3. Scatter plots between SWC and Gs (first row), between VPD and Gs (second row), and between VPD and SWC (third row) at Ne1 site. Temporal scales of the data vary from hourly (leftmost column) to monthly scale (rightmost column). Red dash-line is a linear regression.

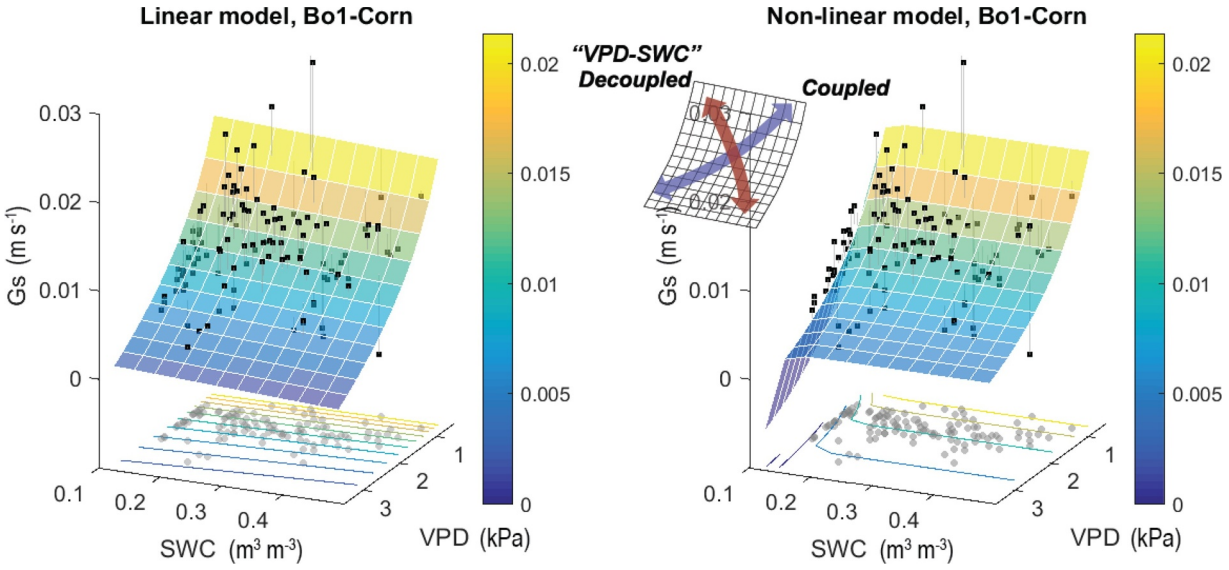

Fig. 4. A surface of the fitted Gs models at Bo1-maize on three-dimensional space of VPD, SWC, and Gs with black dots representing observational data points. Color-coded lines on VPD-SWC plane are contours of Gs, and gray lines and dots are projection lines from the surface and projected points to the plane of VPD-SWC. Color scale and Z-axis redundantly represent Gs for visualization purpose.

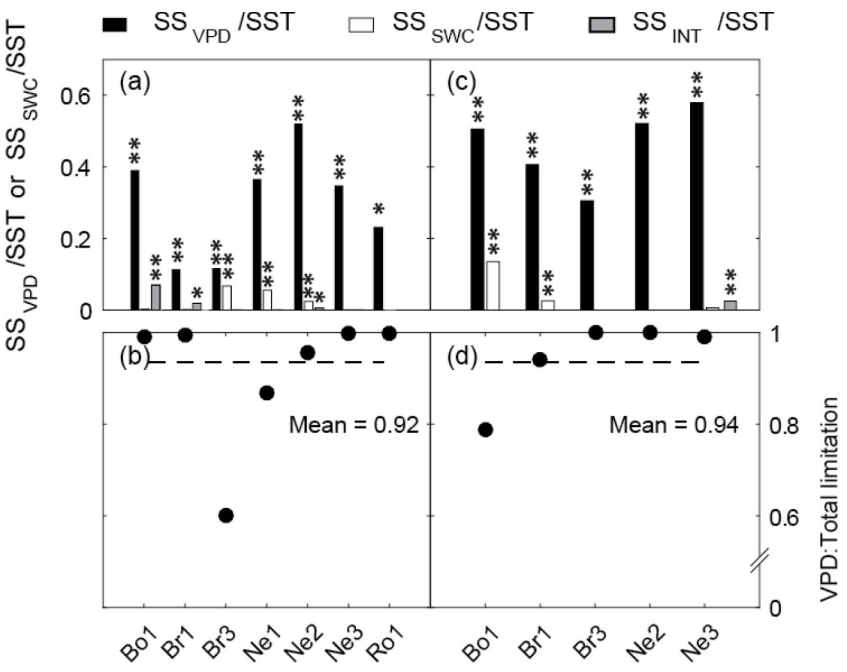

Fig. 5. The upper row shows the fraction of variance in Gs explained by log(VPD), SWC, and interaction terms for each site using the linear model based on Sum of Squares (SS) derived from ANOVA for (a) maize and (c) soybean. The significance level is marked as stars (**: $P < 0.05$, *: $P < 0.1$). The bottom row shows the variance explained by log(VPD) as a fraction of the total variance explained by the linear model. grey dashed line is a mean of the ratios across sites for (b) maize and (d) soybean. Panels (a) and (c) share X axis with (b) and (d), respectively.

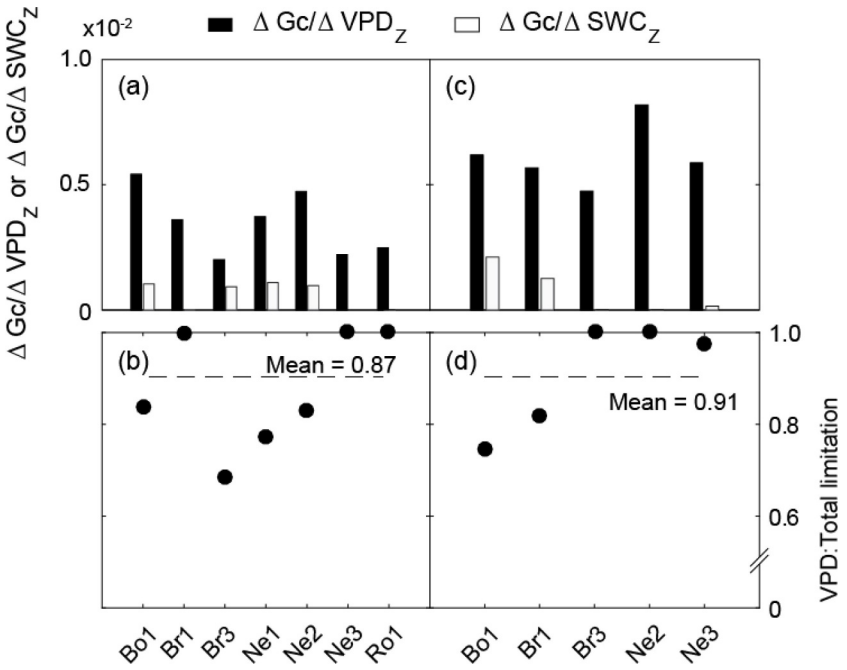

Fig. 6. Same as Fig. 5, but for the non-linear model. Note that this model includes no interaction effect, and contributions of VPD and SWC are derived from partial derivatives of the non-linear model. Calculations of statistical significance were not available for this model. Panels (a) and (c) share X axis with (b) and (d), respectively.

highlighted the dominant contribution of the VPD effect across all the sites, for both models. Specifically, relative contributions of VPD to Gs on average across all the cases were 91% and 89% respectively for the linear and non-linear models (Fig. 5b, d and Fig. 6b, d). We found no clear tendency in attribution results across our environmental gradients ($P > 0.1$ for both mean annual temperature and precipitation). Comparing maize and soybean years, the difference was neither consistent nor significant ($P > 0.1$)). The difference was mostly caused by the difference in Br3, Ne1, and Ne2 sites, where attribution showed a large contrast between maize and soybean. Specifically, relatively large SWC effects were observed at Br3-maize, Ne1-maize, Ne2-maize (linear model: 37%, 13%, and 21%, non-linear model: 32%, 23%, and 17%, respectively at each case), while Br3-soybean and Ne2-soybean did not show much impact from SWC (Table S1). For the linear model, contributions from drivers (VPD, SWC, or interaction) were assumed to be zero for cases where the driver did not have a statistically significant relationship with Gs ($P > 0.05$; based on multiple linear regression; Fig. 5a, 5c). The interaction effect (*SWC*/log · (*VPD*)) was only statistically significant at Bo1-maize and Ne3-soybean, and the effects were small (7% and 3% for the two sites, respectively). Surprisingly, both models consistently showed no significant SWC effect at Ne3-maize or Ne3-soybean. The Ne3 site was not irrigated and had the lowest precipitation of any site (Table 1). The most notable difference between the two models was Bo1-maize, which had a significant SWC effect with the non-linear model but no significant effect with the linear model.

3.4. Approach 3: attribution of GPP variance to VPD and SWC

Wavelet analysis successfully reconstructed wavelet details at the three timescales (time-series data of VPD shown as an example in

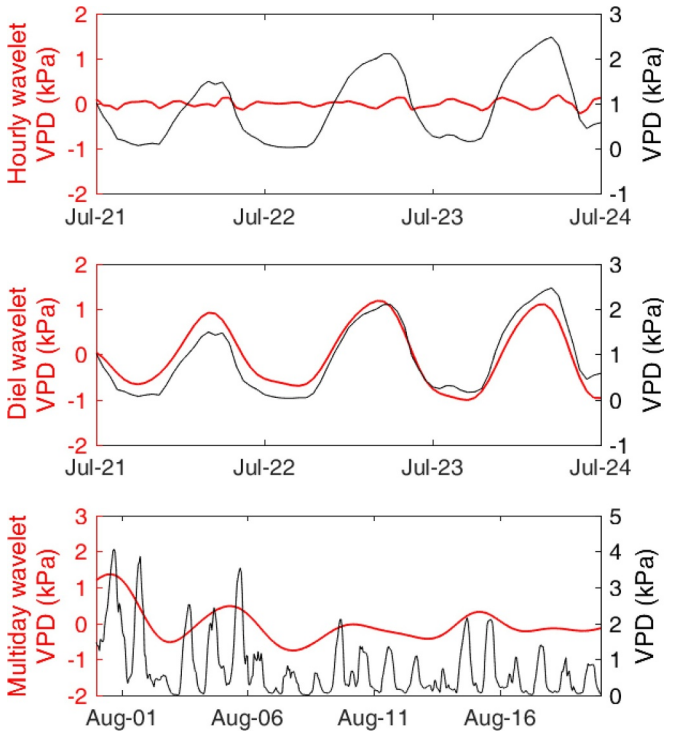

Fig. 7. Example of detailed wavelet reconstruction result for VPD at hourly, diel, and multiday timescales. Black lines are VPD at different time spans, and red lines are reconstructed wavelet.

Fig. 7), and based upon such wavelets, IR attributed most variance of the dependent variable (GPP in this case) to VPD (91%, compared to the sum IR of both VPD and SWC). Among the three timescales, the hourly components of both VPD and SWC in all cases contained only little amount of information about GPP (IR < 0.02; not shown in Fig. 8), but at the other two timescales, $IR_{VPD;GPP}$ has much higher information contents, ranging from 0.18 to 0.3 (Fig. 8). To compare with previous results, the relative fractions of $IR_{VPD;GPP}$ to the sum of $IR_{VPD;GPP}$ and $IR_{SWC;GPP}$ are within 87% - 97% at diel timescale (mean 93%), and 84% - 95% at multiday timescale (mean, 90%). These MI-based results were very similar to the previous results from statistical models. However, here we found a significant relationship between rainfall gradient (i.e., growing season mean precipitation) and $IR_{SWC;GPP}$ (R^2 = 0.45, P < 0.1). IR also revealed a lag effect of VPD and SWC on GPP. At the diel timescale, the most significant lag effect of VPD appeared when the lag was about one day and the increase of IR ranged from 0.07 to 0.13, but not much lag effect of SWC appeared except for Br3 where IR increased by 0.05. At the multiday timescale, considerable SWC lag effect appeared at Bo1, Br1, Br3, and Ro1 with increments of 0.04, 0.11, 0.04, and 0.14, respectively. The majority of such lag effects appeared when the lag was about 2–3 days or up to 8 days at most (in Bo1). Specifically, at Br1 and Ro1, when lag effects were considered, the SWC contribution to GPP was as high as 35%, but still on average, VPD contribution prevailed (85%). At the multiday timescale, the VPD lag effect did not increase IR.

3.5. Path analysis for understanding connectivity among variables

We used a path analysis to identify pathways and their relative importance for explaining impacts of meteorological variables on VPD and SWC. Here we show the path analysis results for the Ne3-soybean case as an example (Fig. 9). The result reveals complex pathways of how PPT and Ta affect Gs through VPD and SWC. At the hourly timescale, PPT, by replenishing soil moisture, positively influences SWC (PV = 0.44) and RH (PV = 0.19), and negatively influences Ta (PV = −0.29). Through land-atmosphere interaction, SWC affects both RH (PV = 0.32) and Ta (PV = −0.04), and subsequently, RH and Ta determine VPD in opposing directions (PV = −0.67 and PV = 0.39, respectively for RH and Ta). Both VPD and SWC then influence Gs (PV = −0.67 and PV = 0.1). At daily timescale, paths are almost the same, but with slight differences. As shown, PPT directly influences Ta and RH that affect VPD, and SWC replenished by precipitation indirectly influences VPD. Eventually, SWC only marginally contributes to Gs, while VPD dominantly contributes to Gs. Although we only show the results here for a single case (i.e. Ne3-soybean in Fig. 9), results from other sites shared similar patterns with only slight differences (Figure S4).

4. Discussion

4.1. How well can empirical models using VPD and SWC explain the variability of stomatal conductance (Gs)?

Our results show that the multiple linear regression model and the non-linear model of Gs both reasonably fit Gs. We are cautious that the flux tower data-derived Gs might deviate from actual Gs, due to the inherent limitations of the derivation method. We further discuss this issue in Section 4.6.

Choice of GS models

We recognize that the model fitting performance might be improved through alternative Gs models. For example, previous studies have shown that incorporating photosynthetic rate into a Gs model can more accurately fit and predict Gs (Ball et al., 1987; Leuning, 1995; Lin et al., 2018; Medlyn et al., 2011). In those models, however, the VPD and SWC impacts on Gs are partially embedded in photosynthetic rate, because photosynthetic rate, as a diffusive flux between leaf and atmospheric boundary layer, is already strongly influenced by Gs (Farquhar et al., 1980; Sharkey et al., 2007). Therefore, our study does not include the GPP in our model, as it may potentially confuse the accurate quantification of the independent impacts of VPD and SWC. Another approach to modeling the influence of VPD and SWC on Gs incorporates VPD as a variable for each soil moisture quantile (Novick et al., 2016; Oren et al., 1999), but these models can only

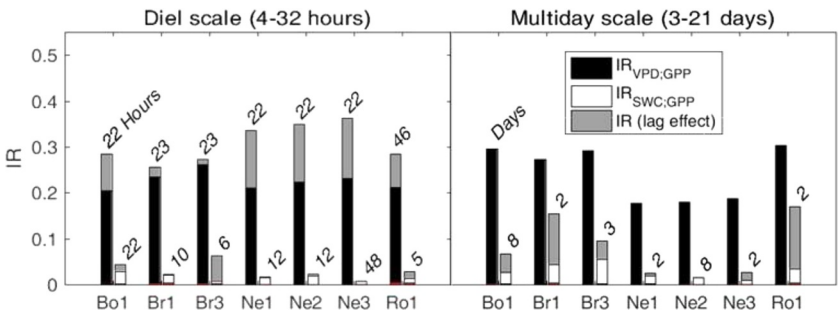

Fig. 8. Relative mutual information between VPD, SWC, and GPP (i.e., IRVPD;GPP and IRSWC;GPP) at diel and multiday timescales. Black and white bars correspond to IRVPD;GPP and IRSWC;GPP, and gray bars indicate increments of IR by introducing time lag effect within the permitted lag range from 0 to 48 h for the diel timescale, and 0 to 10 days for the multiday timescale. The specific lag terms are written at the top of the bars. .

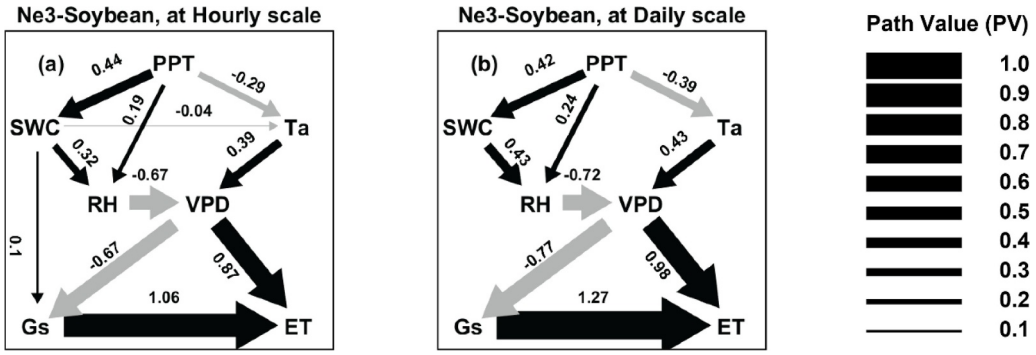

Fig. 9. Path analysis result at (a) the hourly timescale and (b) the daily timescale in Ne3-soybean. Line thickness of arrows represents path value that indicates normalized partial regression coefficient, and gray lines indicate negative effects. Results from other sites can be found in Figure S4. .

incorporate SWC through multiple model fittings at discrete SWC levels. In this case, SWC impact is only quantified from sparse and discrete SWC levels, while VPD impact is quantified from a continuous gradient of VPD. Consequently, the comparison between the two impacts is likely unfair. Based on the above points, we chose to model Gs using continuous functions of VPD and SWC with two different models in which we can treat VPD and SWC equally within a single framework and compare their contributions, which is more suitable for our goal compared with other prior models.

4.2. How much does VPD or SWC contribute to plant water stress in croplands?

Our analyses attribute most Gs variance to VPD variations, and this finding holds true with little dependence on variation in environmental conditions (rainfall and temperature gradients), crop types (maize vs. soybean), and management practices (whether irrigated or not). Both Gs and VPD show a clear diurnal pattern, which may result in a greater correlation between Gs and VPD, compared to the correlation between Gs and SWC. To avoid such an apparent correlation in comparing impacts of VPD and SWC on Gs, we conducted attribution analyses at daily and multi-daily timescales, but at both timescales, VPD impact on Gs was dominant. Significant lag effects of VPD and SWC on GPP emerge at some instances significantly changing the attribution result at some sites, but even considering lag effects, the overall dominance of VPD contribution (85%) on GPP still holds. Rainfall gradient is only weakly related to soil moisture impact from the information theory-based approach, and other than that, both rainfall and temperature gradients have no significant impact on the results. Although we find differences in averaged attributions between crop types and management practice, such differences are not consistent across the cases and are not statistically significant ($P > 0.1$). Here, we acknowledge that the result about GPP might not be exactly interpreted as those about Gs. However, Gs determines the supply of CO_2 and thus substantially influence GPP. Therefore, we believe the relationships between VPD, SWC, and GPP would be mostly transferable to the relationships between VPD, SWC, and Gs. Besides, the mutual information result, as described above, shows that both VPD and SWC contribute to GPP in a very similar manner as observed for the other two analytical methods.

There is growing evidence supporting dominant role of VPD in controlling Gs

Our attribution result is consistent with prior work, e.g. Lobell et al. (2014, 2013) which indicated high VPD as a primary reason of crop water stress that leads to crop yield loss in the Midwest U.S., although they did not fully identify underlying plant hydrological mechanisms. Lobell et al. (2013, 2014) also suggested that the high correlation between temperature and crop yield is largely driven by the direct impact of VPD on crop productivity and less so by direct temperature effects on crops (Ainsworth and Ort, 2010; Schlenker and Roberts, 2009). The high correlation between VPD and temperature leads to the above apparently confounding relationships. Recent work by Lin et al. (2018) shows a similar finding of dominant VPD impacts at the diel scale using flux tower data for U.S. croplands. Additionally, studies of other biomes have identified dominant contributions of VPD on Gs and consequential plant-atmosphere fluxes of CO_2 and H_2O (Novick et al., 2016; Sulman et al., 2016). The strong dependence of Gs on VPD also confirms existing understanding of the pronounced relationship between Gs and VPD (Medlyn et al., 2011; Monteith, 1965; Oren et al., 1999).

4.3. How can the dominant VPD impact be reconciled with previous studies on agricultural droughts?

There have been many studies quantifying the impact and severity of agricultural droughts by using precipitation, largely as a proxy of soil moisture status (A. K. Mishra and Singh, 2010; Palmer, 1965). Accumulated evidence of the strong explanatory ability of precipitation for agricultural droughts supports the importance of soil water supply in determining agricultural drought impact and severity. However, our attribution results show that VPD plays a dominant role in regulating Gs and very likely in agricultural droughts as well, which at first glance may contradict prior understanding but is in line with recent studies (Lin et al., 2018; Novick et al., 2016; Sulman et al., 2016).

One key to the reconciliation of the two apparently opposing lines of evidence lies in the interpretation of the strong impacts of precipitation and SWC on agricultural droughts. Here, we conducted a path analysis to resolve the apparent disagreement between the current work and previous knowledge about agricultural drought. The path analysis revealed that precipitation influences SWC and, subsequently, Ta and RH through land-atmosphere interactions (i.e., SWC impact on RH and Ta). Both RH and Ta dominantly determine VPD, which subsequently exerts a strong control on Gs. Therefore, the previously reported high correlation between precipitation and agricultural drought impact is only partially realized by the direct soil moisture impact, while the strongest influence occurs through the indirect effect of SWC on VPD, at least for the U.S. Corn Belt. A timescale difference can provide a further reconciliation between the previous understanding of agricultural drought and our result. At monthly to yearly timescales, VPD and SWC are more tightly coupled (Fig. 3), so previous agricultural drought studies in which data were analyzed on monthly or yearly timescales (Panu and Sharma, 2002) may have simultaneously incorporated co-occurring effects of both VPD and SWC.

4.4. Uncertainties in methods and results

Gs derivation

The flux tower data-derived Gs might deviate from actual Gs, due to the inherent limitations of the derivation method. Using the inverted

Penman-Monteith equation to calculate Gs assumes that flux measurements are estimates of transpiration while in reality eddy-covariance measurements include the combination of transpiration and soil evaporation. However, we adopted various data selection criteria in this study, including limiting the analysis to the peak growing season, excluding data within two days after every precipitation and irrigation event, and excluding periods of low SR_{in} (<500 Wm^{-2}). These data filters should minimize bias due to evaporation from the soil and leaf surfaces by excluding rainwater evaporation, plant surface dew formation/evaporation, and soil evaporation from ET (Knauer et al., 2017).

SWC as a proxy of soil moisture condition

The depth of the SWC measurements might be one factor that could reduce the apparent contribution of SWC to variance in Gs. The SWC data used here are from the top soil layer (10–25 cm), and may differ from SWC of the aggregated root zone, so we further tested differences in temporal patterns of SWC at multiple soil layers by using data measured near the location of the Bo1 site from 2012 to 2017 (Water and Atmospheric Resources Monitoring Program of the Illinois State Water Survey). Among temporal patterns of SWC of multiple depths (20 cm, 50 cm, 100 cm, and 150 cm) during a period from July to August only the deeper soils (100 cm and 150 cm) showed different patterns from the top layer SWC (10 cm depth) as supported by literature (Hupet and Vanclooster, 2002; Tromp-van Meerveld and McDonnell, 2006) (Figure S5). Considering a typical vertical distribution of root biomass where roughly two thirds is in the upper 30 cm, even though maximal rooting depth can be more than 100 cm deep, SWC depth is unlikely to be a critical uncertainty in our result (Fan et al., 2016; J. Zhang and Davies, 1989).

Using SWC may underestimate the contribution of soil moisture deficit to Gs variability because SWC variation above the field capacity lead to little variation in both SWP and plant responses (Chapin III, Matson, and Mooney, 2006) while SWP better represent soil moisture condition from the plants' perspective. Unfortunately, SWP data are not available from our study sites, and empirical or semi-empirical conversion from SWC to SWP possibly involves large uncertainties, as the relation between SWC and SWP is non-linear and soil property-dependent. We thus indirectly incorporated such non-linear relation between SWC and SWP by fitting a site-specific non-linear model between SWC and Gs, and we believe this approach can implicitly embed a conversion from SWC to SWP without introducing additional uncertainties.

The severity of dryness

The severity of dryness that these sites experienced is another factor that may affect the attribution results. Due to the limited length of the data records, our data only contains limited samples for extremely dry years (e.g., 2012), and the majority of our data were under more normal climate conditions similarly to Lin et al. (2018). This lack of data from extremely dry conditions in our sample may partially explain the marginal contribution of SWC in our statistical models. Previous analyses have shown that the contribution of SWC to Gs is the strongest when soils are very dry (Sulman et al., 2016). Even for some cases that include an extremely dry year (2012), Gs responses to VPD and SWC captured by the models may have been biased towards the responses under normal conditions due to the low occurrence of extremely dry conditions. Therefore, we conducted additional analysis to explore whether there is any SWC effect that may not be captured by the model, by comparing distributions of Gs between dry and normal SWC conditions coinciding with similar ranges of VPD, but we did not find any clear SWC effects from the comparison of the Gs distributions (Figure S6). Nevertheless, we acknowledge that SWC might have greater contributions at sites with more severe soil drying than those observed in this study (See Figure S7 for hourly SWC data histograms from the study sites).

4.5. Spatial representativeness of the study

The study includes seven flux tower sites that are representative of the general U.S. Corn Belt conditions, and therefore, the data and findings of our study are representative of the majority of the U.S. Corn Belt. Specifically, studied sites are from a range of climatic gradient as shown by the coverage of the precipitation gradient (Fig. 1b). Despite some potential exceptional conditions in Nebraska, the data can represent most areas in the Corn Belt, which is shown by the corn-planted acreage map (Farm Service Agency of the United States Department of Agriculture; Fig. 1b). Additionally, it is worth mentioning that U.S. Corn Belt is generally wet for its summertime, and this is also why the vast majority of the U.S. Corn Belt croplands ($>90\%$) are rainfed - which means that they are exposed to interannual variability of climate (Fig. 1c). 5 out of the 7 sites from our study are rainfed, and the rest 2 sites (Mead Nebraska) are irrigated when necessary, but not frequent at all as this site is not dry enough. For very dry regions in the U.S. Corn Belt (e.g. western Nebraska), croplands are almost all irrigated and thus not the major focus of this study. Finally, our study has included the 2012 record at some sites, and 2012 is the worst drought of the past several decades in the U.S. Corn Belt, which further supports representativeness of the data. Based on the above reasons, we are fully convinced that our study is representative of the general U.S. Corn Belt conditions, especially for the rainfed croplands (92% majority of the production region, our major focus); and the rest 8% is irrigated, where water stress is much less an issue.

4.6. Prospective progression under climate change

With regards to ongoing climatic changes, air temperature and VPD are expected to continue to increase as a result of both increased temperature and decreased relative humidity over continents (Byrne and O'Gorman, 2016; Ficklin and Novick, 2017; Wuebbles et al., 2017). VPD may increase hydrological stress and suppress Gs to an increasingly severe degree (Dai et al., 2004; Nicholls, 2004; Novick et al., 2016). We thus would expect a further intensification of detrimental effects on plant growth induced by higher VPD in U.S. Corn Belt agroecosystems, which would lead to further crop yield loss in the U.S. Corn Belt (Lobell et al., 2014; Novick et al., 2016) or possibly an increase in irrigation area and intensity (DeLucia et al., 2019). At the same time, due to the strong VPD impact on Gs, VPD can serve as a strong indicator of water stress on Gs for maize and soybean in the U.S. Corn Belt. This is especially true at longer timescales such as monthly and yearly timescale. As higher VPD and lower SWC commonly co-occur, VPD would be able to explain the majority of Gs variance and to quantify agricultural droughts.

5. Conclusions

Our study used two different empirical models and an information theory-based approach to partition the contributions of VPD and SWC to Gs (or GPP for the third approach) variance and investigated which factor is the most responsible for agricultural drought impacts in the U.S. Corn Belt. Previous drought studies in the agricultural domain mostly relied on climate variables such as precipitation and air temperature not only because these climate data cover long time periods over large areas, but also because other critical field data (such as soil moisture, vapor pressure deficit, ecosystem fluxes of CO_2 and H_2O) were not sufficiently available to investigate the underlying mechanism of drought. Subsequently, our conventional understanding of agricultural drought was not clearly linked to plant physiology. However, this study focuses on a mechanical perspective of stomatal regulation and attributes Gs variance to the hydrological variables that directly define plant water stress, VPD and SWC. By investigating the stomatal response to both these environmental factors, this study provides a process-based understanding of agricultural drought that contrasts with

previous assessments that focused solely on the role of soil moisture. Based on our results, we find that VPD dominates Gs variability compared to soil moisture across multiple agroecosystems analyzed here, although explained variance varies modestly from site to site. Our findings imply that current precipitation-based measures for quantifying agricultural drought severity or impact might be inappropriate, as our path analysis indicates that precipitation affects both SWC and VPD variability, and only has a modest correlation with VPD, which dominantly controls Gs variability. We thus suggest that VPD might be a better indicator to assess the drought impact on agroecosystems in the U.S. Corn Belt than precipitation, though further in-depth analysis is still needed to confirm our findings.

Declaration of Competing Interest

The authors declare that they have no known competing financial interests or personal relationships that could have appeared to influence the work reported in this paper.

Acknowledgements

Guan and Kimm acknowledge financial support from NASA New Investigator Award and NASA Carbon Monitoring System Award (NNX16AI56G, 80NSSC18K0170) managed through the NASA Terrestrial Ecology Program, and the Illinois Water Resources Center (IWRC) affiliated to the US Geological Survey (USGS). Guan also acknowledges the supports from USDA National Institute of Food and Agriculture (NIFA) grant (2017-67013-26253). Gentine acknowledges funding from DOE Early Career grant. Any opinions, findings, and conclusions or recommendations expressed in this publication are those of the author(s) and do not necessarily reflect the views of the U.S. Department of Agriculture. Mention of trade names or commercial products in this publication is solely for the purpose of providing specific information and does not imply recommendation or endorsement by the U.S. Department of Agriculture. USDA is an equal opportunity provider and employer.

Supplementary materials

Supplementary material associated with this article can be found, in the online version, at doi:10.1016/j.agrformet.2020.107930.

Reference

Ainsworth, E.A., Ort, D.R., 2010. How do we improve crop production in a warming world. Plant. Physiol. 154 (2) 526 LP – 530Retrieved from. http://www.plantphysiol.org/content/154/2/526.abstract.

Allen, R.G., Luis, S.P., RAES, D., Smith, M., 1998. FAO irrigation and drainage paper no. 56. Crop Evapotranspiration (guidelines for computing crop water requirements). Irrigat. and Drainage.

Anderson, M.C., Hain, C., Wardlow, B., Pimstein, A., Mecikalski, J.R., Kustas, W.P., 2010. Evaluation of drought indices based on thermal remote sensing of evapotranspiration over the continental united states. J. Clim. 24 (8), 2025–2044. https://doi.org/10.1175/2010JCLI3812.1.

Ball, J.T., Woodrow, I.E., Berry, J.A., 1987. In: Biggins, J. (Ed.), Springer, DordrechtNetherlands, pp. 221–224. https://doi.org/10.1007/978-94-017-0519-6_48.

Brunsell, N.A., Anderson, M.C., 2011. Characterizing the multi–scale spatial structure of remotely sensed evapotranspiration with information theory. Biogeosciences 8 (8), 2269–2280. https://doi.org/10.5194/bg-8-2269-2011.

Byrne, M.P., O'Gorman, P.A., 2016. Understanding decreases in land relative humidity with global warming: conceptual model and GCM simulations. J. Clim. 29 (24), 9045–9061. https://doi.org/10.1175/JCLI-D-16-0351.1.

Cammalleri, C., Anderson, M.C., Kustas, W.P., 2014. Upscaling of evapotranspiration fluxes from instantaneous to daytime scales for thermal remote sensing applications. Hydrol. Earth Syst. Sci. 18 (5), 1885–1894. https://doi.org/10.5194/hess-18-1885-2014.

Chang, F.-C., Wallace, J.M., 1987. Meteorological conditions during heat waves and droughts in the United States Great plains. Month. Weather Rev. 115 (7), 1253–1269 10.1175/1520-0493(1987)115<1253:MCDHWA>2.0.CO;2.

Chapin III, S.F., Matson, P.A., Mooney, H.A., 2006. *Principles of Terrestrial Ecosystem Ecology. Principles of Terrestrial Ecosystem Ecology*. New York. Springer, NY, USANew York. https://doi.org/10.1007/0-387-21663-4_6.

Chaves, M.M., Maroco, J.P., Pereira, J.S., 2003. Understanding plant responses to drought — from genes to the whole plant. Funct. Plant Biol. 30 (3), 239–264. https://doi.org/10.1071/FP02076. Retrieved from.

Dai, A., Trenberth, K.E., Qian, T., 2004. A global dataset of palmer drought severity index for 1870–2002: relationship with soil moisture and effects of surface warming. J. Hydrometeorol. 5 (6), 1117–1130. https://doi.org/10.1175/JHM-386.1.

Davies, W.J., Zhang, J., 1991. Root signals and the regulation of growth and development of plants in drying soil. Annu. Rev. Plant Physiol. Plant Mol. Biol. 42 (1), 55–76. https://doi.org/10.1146/annurev.pp.42.060191.000415.

DeLucia, E.H., Chen, S., Peng, B., Guan, K., Gomez-Casanovas, N., Kantola, I.B., Ort, D.R., 2019. Are we approaching a water ceiling to yield in rain fed agriculture of the United States. Ecosphere 10 (6). https://doi.org/10.1002/ecs2.2773.

Dietze, M.C., Vargas, R., Richardson, A.D., Stoy, P.C., Barr, A.G., Anderson, R.S., Weng, E., 2011. Characterizing the performance of ecosystem models across time scales: a spectral analysis of the North American Carbon Program site-level synthesis. J. Geophys. Res. 116 (G4), 2005–2012. https://doi.org/10.1029/2011JG001661.

Fan, J., McConkey, B., Wang, H., Janzen, H., 2016. Root distribution by depth for temperate agricultural crops. Field Crops. Res. 189, 68–74. https://doi.org/10.1016/j.fcr.2016.02.013.

FAO, 2013. FAO Statistical Databases Retrieved from http://faostat.fao.org.

Farquhar, G.D., von Caemmerer, S., Berry, J.A., 1980. A biochemical model of photosynthetic CO2 assimilation in leaves of C3 species. Planta 149 (1), 78–90. https://doi.org/10.1007/BF00386231.

Fassbinder, J.J., Griffis, T.J., Baker, J.M., 2012. Interannual, seasonal, and diel variability in the carbon isotope composition of respiration in a C3/C4 agricultural ecosystem. Agric. For. Meteorol. 153, 144–153. https://doi.org/10.1016/j.agrformet.2011.09.018.

Ficklin, D.L., Novick, K.A., 2017. Historic and projected changes in vapor pressure deficit suggest a continental-scale drying of the United States atmosphere. J. Geophys. Res. https://doi.org/10.1002/2016JD025855.

Gentine, P., Chhang, A., Rigden, A., Salvucci, G., 2016. Evaporation estimates using weather station data and boundary layer theory. Geophys. Res. Lett. 43 (22). https://doi.org/10.1002/2016GL070819.

Gollan, T., Schurr, U., Schulze, E.-D., 1992. Stomatal response to drying soil in relation to changes in the xylem sap composition of Helianthus annuus. I. The concentration of cations, anions, amino acids in, and pH of, the xylem sap. Plant. Cell Environ. 15 (5), 551–559. https://doi.org/10.1111/j.1365-3040.1992.tb01488.x.

Green, J.K., Konings, A.G., Alemohammad, S.H., Berry, J.A., Entekhabi, D., Kolassa, J., Gentine, P., 2017. Regionally strong feedbacks between the atmosphere and terrestrial biosphere. Nature Geosci. 10 (6), 410–414. https://doi.org/10.1038/ngeo2957. Retrieved from.

Guan, K., Thompson, S.E., Harman, C.J., Basu, N.B., Rao, P.S.C., Sivapalan, M., Kalita, P.K., 2011. Spatiotemporal scaling of hydrological and agrochemical export dynamics in a tile-drained Midwestern watershed. Water Resour. Res. 47 (10). https://doi.org/10.1029/2010WR009997.

Guan, K., Berry, J.A., Zhang, Y., Joiner, J., Guanter, L., Badgley, G., Lobell, D.B., 2016. Improving the monitoring of crop productivity using spaceborne solar-induced fluorescence. Glob. Chang. Biol 22 (2), 716–726. https://doi.org/10.1111/gcb.13136.

Heim, R.R., 2002. A review of twentieth-century drought indices used in the United States. Bull. Am. Meteorol. Soc. 83 (8), 1149–1165. https://doi.org/10.1175/1520-0477-83.8.1149.

Huang, C.-W., Domec, J.-C., Ward, E.J., Duman, T., Manoli, G., Parolari, A.J., Katul, G.G., 2016. The effect of plant water storage on water fluxes within the coupled soil–plant system. New Phytologist 213 (3), 1093–1106. https://doi.org/10.1111/nph.14273.

Hupet, F., Vanclooster, M., 2002. Intraseasonal dynamics of soil moisture variability within a small agricultural maize cropped field. J. Hydrol. (Amst) 261 (1), 86–101. https://doi.org/10.1016/S0022-1694(02)00016-1.

Katul, G.G., Oren, R., Manzoni, S., Higgins, C., Parlange, M.B., 2012. Evapotranspiration: a process driving mass transport and energy exchange in the soil-plant-atmosphere-climate system. Rev. Geophys. 50 (3). https://doi.org/10.1029/2011RG000366. n/a–n/a.

Knauer, J., Zaehle, S., Medlyn, B.E., Reichstein, M., Williams, C.A., Migliavacca, M., Linderson, M., 2017. Towards physiologically meaningful water-use efficiency estimates from eddy covariance data. Glob. Chang. Biol. https://doi.org/10.1111/gcb.13893.

Kumar, P., Ruddell, B.L., 2010. Information driven Ecohydrologic self-organization. Entropy 12 (10), 2085–2096. https://doi.org/10.3390/e12102085.

Leuning, R., 1995. A critical appraisal of a combined stomatal-photosynthesis model for C3 plants. Plant. Cell Environ. 18 (4), 339–355. https://doi.org/10.1111/j.1365-3040.1995.tb00370.x.

Li, C.C., 1975. *Path Analysis - a primer*.Pacific Grove. The Boxwood Press, California.

Lin, C., Gentine, P., Huang, Y., Guan, K., Kimm, H., Zhou, S., 2018. Diel ecosystem conductance response to vapor pressure deficit is suboptimal and independent of soil moisture. Agric. For. Meteorol 250–251. https://doi.org/10.1016/j.agrformet.2017.12.078. 24–34.

Lobell, D.B., Hammer, G.L., McLean, G., Messina, C., Roberts, M.J., Schlenker, W., 2013. The critical role of extreme heat for maize production in the united states. Nat. Clim. Chang. 3, 497. https://doi.org/10.1038/nclimate1832. Retrieved from.

Lobell, D.B., Roberts, M.J., Schlenker, W., Braun, N., Little, B.B., Rejesus, R.M., Hammer, G.L., 2014. Greater sensitivity to drought accompanies maize yield increase in the U.S. Midwest. Science 344 (6183) 516 LP – 519Retrieved from. http://science.sciencemag.org/content/344/6183/516.abstract.

Lohammar, T., Larsson, S., Linder, S., Falk, S.O., 1980. FAST: simulation models of

gaseous exchange in scots pine. Ecol. Bull. (32), 505–523. Retrieved from. http://www.jstor.org/stable/20112831.
Mallat, S.G., 1989. A theory for multiresolution signal decomposition: the wavelet representation. IEEE Trans. Pattern Anal. Mach. Intell. 11, 674–693. https://doi.org/10.1109/34.192463.
Martínez-Vilalta, J., Poyatos, R., Aguadé, D., Retana, J., Mencuccini, M., 2014. A new look at water transport regulation in plants. New Phytologist 204 (1), 105–115. https://doi.org/10.1111/nph.12912.
Medlyn, B.E., Duursma, R.A., Eamus, D., Ellsworth, D.S., Prentice, I.C., Barton, C.V.M., Wingate, L., 2011. Reconciling the optimal and empirical approaches to modelling stomatal conductance. Glob. Chang Biol. 17 (6), 2134–2144. https://doi.org/10.1111/j.1365-2486.2010.02375.x.
Meyers, T.P., Hollinger, S.E., 2004. An assessment of storage terms in the surface energy balance of maize and soybean. Agric. For. Meteorol 125 (1), 105–115. https://doi.org/10.1016/j.agrformet.2004.03.001.
Mishra, A.K., Singh, V.P., 2010. A review of drought concepts. J. Hydrol. (Amst) 391 (1), 202–216. https://doi.org/10.1016/j.jhydrol.2010.07.012.
Mishra, V., Cherkauer, K.A., Shukla, S., 2010. Assessment of drought due to historic climate variability and projected future climate change in the Midwestern United States. J. Hydrometeorol. 11 (1), 46–68. https://doi.org/10.1175/2009JHM1156.1.
Monteith, J.L., 1965. Evaporation and environment. Symp. Soc. Exp. Biol. 19, 205–224.
Monteith, J.L., 1995. A reinterpretation of stomatal responses to humidity. Plant Cell Environ. 18 (4), 357–364. https://doi.org/10.1111/j.1365-3040.1995.tb00371.x.
Nicholls, N., 2004. The changing nature of Australian droughts. Climat. Change 63 (3), 323–336. https://doi.org/10.1023/B:CLIM.0000018515.46344.6d.
Novick, K.A., Ficklin, D.L., Stoy, P.C., Williams, C.A., Bohrer, G., Oishi, A.C., Phillips, R.P., 2016. The increasing importance of atmospheric demand for ecosystem water and carbon fluxes. Nature Clim. Change 6, 1023–1027. https://doi.org/10.1038/nclimate3114. Retrieved from.
Oren, R., Sperry, J.S., Katul, G.G., Pataki, D.E., Ewers, B.E., Phillips, N., Schäfer, K.V.R., 1999. Survey and synthesis of intra- and interspecific variation in stomatal sensitivity to vapour pressure deficit. Plant Cell Environ. 22 (12), 1515–1526. https://doi.org/10.1046/j.1365-3040.1999.00513.x.
Palmer, W.C., 1965. *Meteorological drought.* U.S. *Weather Bureau.* Res. Paper No.45.
Panu, U.S., Sharma, T.C., 2002. Challenges in drought research: some perspectives and future directions. Hydrol. Sci. J. 47, S19–S30. https://doi.org/10.1080/02626660209493019. sup1.
Percival, D.B., Walden, A.T., 2000. Wavelet Methods for Time Series Analysis. Cambridge Series in Statistical and Probabilistic Mathematics. Cambridge University Press, Cambridge. https://doi.org/10.1017/CBO9780511841040.
Percival, D.P., 1995. On estimation of the wavelet variance. Biometrika 82 (3), 619–631. https://doi.org/10.2307/2337538.
Peterson, T.C., Hoerling, M.P., Stott, P.A., Herring, S.C., 2013. Explaining extreme events of 2012 from a Climate perspective. Bull. Am. Meteorol. Soc. 94 (9), S1–S74. https://doi.org/10.1175/BAMS-D-13-00085.1.
Reichstein, M., Moffat, A.M., & Sickel, T.W. (2017). REddyProc: data processing and plotting utilities of (half-) hourly eddy-covariance measurements. Retrieved fromhttps://r-forge.r-project.org/projects/reddyproc/.
Ruddell, B.L., Sturtevant, M., Kang, M., & Yu, R. (2008). ProcessNetwork Software, version 1.5. [Available athttp://www.mathworks.com/matlabcentral/fileexchange/41515-processnetwork-version-1-5-software].
Sadras, V.O., Milroy, S.P., 1996. Soil-water thresholds for the responses of leaf expansion and gas exchange: a review. Field Crops. Res. 47 (2), 253–266. https://doi.org/10.1016/0378-4290(96)00014-7.
Sakai, T., Iizumi, T., Okada, M., Nishimori, M., Grünwald, T., Prueger, J., Ceschia, E., 2016. Varying applicability of four different satellite-derived soil moisture products to global gridded crop model evaluation. Int. J. Appl. Earth Observ. Geoinf. 48, 51–60. https://doi.org/10.1016/j.jag.2015.09.011.
Schlenker, W., Roberts, M.J., 2009. Nonlinear temperature effects indicate severe damages to U.S. crop yields under climate change. Proc. Natl. Acad. Sci. 106 (37), 15594–15598. Retrieved from. http://www.pnas.org/content/106/37/15594.abstract.
Shannon, C.E., 1948. A mathematical theory of communication. Bell Syst. Tech. J. 27 (3), 379–423. https://doi.org/10.1002/j.1538-7305.1948.tb01338.x.
Sharkey, T.D., Bernacchi, C.J., Farquhar, G.D., Singsaas, E.L., 2007. Fitting photosynthetic carbon dioxide response curves for C3 leaves. Plant Cell Environ. 30 (9), 1035–1040. https://doi.org/10.1111/j.1365-3040.2007.01710.x.
Stoy, P.C., Williams, M., Spadavecchia, L., Bell, R.A., Prieto-Blanco, A., Evans, J.G., van Wijk, M.T., 2009. Using information theory to determine optimum pixel size and shape for ecological studies: aggregating land surface characteristics in arctic ecosystems. Ecosystems 12 (4), 574–589. https://doi.org/10.1007/s10021-009-9243-7.
Stoy, P.C., Katul, G., Siqueira, G., Juang, M.B.S., McCarthy, J.-Y., Kim, H.R., Oren R., H.-S., 2005. Variability in net ecosystem exchange from hourly to inter-annual time scales at adjacent pine and hardwood forests: a wavelet analysis. Tree Physiol. 25 (7), 887–902. https://doi.org/10.1093/treephys/25.7.887. Retrieved from.
Sturtevant, C., Ruddell, B.L., Knox, S.H., Verfaillie, J., Matthes, J.H., Oikawa, P.Y., Baldocchi, D.D., 2016. Identifying scale-emergent, nonlinear, asynchronous processes of wetland methane exchange. J. Geophys. Res. 121 (1), 188–204. https://doi.org/10.1002/2015JG003054.
Sulman, B.N., Roman, D.T., Yi, K., Wang, L., Phillips, R.P., Novick, K.A., 2016. High atmospheric demand for water can limit forest carbon uptake and transpiration as severely as dry soil. Geophys. Res. Lett. 43, 9686–9695. https://doi.org/10.1002/2016GL069416.
Suyker, A.E., Verma, S.B., Burba, G.G., Arkebauer, T.J., Walters, D.T., Hubbard, K.G., 2004. Growing season carbon dioxide exchange in irrigated and rainfed maize. Agric. For. Meteorol. 124 (1), 1–13. https://doi.org/10.1016/j.agrformet.2004.01.011.
Taiz, L., Zeiger, E., Moller, I.M., Murphy, A., 2014. *Plant physiology* (Sixth). Sinauer Assoc.
Trenberth, K.E., Branstator, G.W., Arkin, P.A., 1988. Origins of the 1988 North American Drought. Science 242 (4886), 1640–1645. Retrieved from. http://science.sciencemag.org/content/242/4886/1640.abstract.
Tromp-van Meerveld, H.J., McDonnell, J.J., 2006. On the interrelations between topography, soil depth, soil moisture, transpiration rates and species distribution at the hillslope scale. Adv. Water Resour 29 (2), 293–310. https://doi.org/10.1016/j.advwatres.2005.02.016.
Wilhite, D.A., Glantz, M.H., 1985. Understanding: the drought phenomenon: the role of definitions. Water Int. 10 (3), 111–120. https://doi.org/10.1080/02508068508686328.
Wu, J., Guan, K., Hayek, M., Restrepo-Coupe, N., Wiedemann, K.T., Xu, X., Saleska, S.R., 2016. Partitioning controls on Amazon forest photosynthesis between environmental and biotic factors at hourly to interannual timescales. Glob. Chang Biol. 23 (3), 1240–1257. https://doi.org/10.1111/gcb.13509.
Wuebbles, D.J., Fahey, D.W., Hibbard, K.A., Dokken, D.J., Stewart, B.C., T.K., M., 2017. 2017. Climate science special report. Fourth Natl. Climate Assess. I. https://doi.org/10.7930/j0j964j6.
Wutzler, T., Lucas-Moffat, A., Migliavacca, M., Knauer, J., Sickel, K., Šigut, L., Reichstein, M., 2018. Basic and extensible post-processing of eddy covariance flux data with REddyProc. Biogeosciences 15 (16), 5015–5030. https://doi.org/10.5194/bg-15-5015-2018.
Zhang, J., Davies, W.J., 1989. Abscisic acid produced in dehydrating roots may enable the plant to measure the water status of the soil. Plant Cell Environ. 12 (1), 73–81. https://doi.org/10.1111/j.1365-3040.1989.tb01918.x.
Zhang, Z., Telesford, Q.K., Giusti, C., Lim, K.O., Bassett, D.S., 2016. Choosing wavelet methods, filters, and lengths for functional brain network construction. PLoS ONE 11 (6), e0157243. https://doi.org/10.1371/journal.pone.0157243.